



DR DANIEL PISERA (Orcid ID : 0000-0001-8795-1551)

Article type : Original Article

Anterior Pituitary gland synthesizes Dopamine from L-3,4-dihydroxyphenylalanine (L-Dopa)

Santiago Jordi Orrillo¹, Nataly de Dios¹, Antonela Sofía Asad¹, Fernanda De Fino², Mercedes Imsen¹, Ana Clara Romero¹, Sandra Zárate¹, Jimena Ferraris¹, Daniel Pisera¹

¹Instituto de Investigaciones Biomédicas (INBIOMED, UBA-CONICET), Facultad de Medicina, Universidad de Buenos Aires, Buenos Aires, Argentina

²Instituto de Investigaciones Farmacológicas (ININFA, UBA-CONICET), Facultad de Farmacia y Bioquímica, Universidad de Buenos Aires, Buenos Aires, Argentina.

Short title: “Dopamine synthesis by Anterior Pituitary”

Corresponding author

Daniel Pisera

INBIOMED, UBA - CONICET

Facultad de Medicina, Universidad de Buenos Aires

Paraguay 2155, piso 10

Ciudad de Buenos Aires, C1121ABG, Argentina

Tel: +54 11 52853378 (53378)

E-Mail: dpisera@fmed.uba.ar

Keywords: L-Dopa, Aromatic L-amino acid decarboxylase (AADC), Anterior pituitary, Dopamine, AtT20 cells, GH3 cells.

Abstract

Prolactin (PRL) is a hormone principally secreted by lactotrophs of the anterior pituitary gland. Although the synthesis and exocytosis of this hormone are mainly under the regulation of hypothalamic dopamine (DA), the possibility that the anterior pituitary synthesizes this catecholamine remains unclear. In this study, our aim was to determine if the anterior pituitary produces DA from the precursor L-Dopa. To this purpose, we studied the expression of aromatic L-amino acid decarboxylase (AADC) enzyme and the transporter VMAT2 in the anterior pituitary, AtT20 and GH3 cells by immunofluorescence and western blot. Moreover, we investigated the production of DA

This article has been accepted for publication and undergone full peer review but has not been through the copyediting, typesetting, pagination and proofreading process, which may lead to differences between this version and the [Version of Record](#). Please cite this article as [doi: 10.1111/JNE.12885](https://doi.org/10.1111/JNE.12885)

This article is protected by copyright. All rights reserved

Accepted Article

from L-Dopa and its release *in vitro*. Then, we explored the effects of L-Dopa in the secretion of PRL from anterior pituitary fragments. We observed that the anterior pituitary, AtT20 and GH3 cells express both AADC and VMAT2. Next, we detected an increase in DA content after anterior pituitary fragments were incubated with L-Dopa. Also, the presence of L-Dopa increased DA levels in incubation media and reduced PRL secretion. Likewise, the content of cellular DA increased after AtT20 cells were incubated with L-Dopa. In addition, L-Dopa reduced CRH-stimulated ACTH release from these cells after AADC activity was inhibited by NSD-1015. Moreover, DA formation from L-Dopa increased apoptosis and decreased proliferation. However, in the presence of NSD-1015, L-Dopa decreased apoptosis and increased proliferation rates. These results suggest that the anterior pituitary synthesizes DA from L-Dopa by AADC and this catecholamine can be released from this gland contributing to the control of PRL secretion. In addition, our results suggest that L-Dopa exerts direct actions independently from its metabolism to DA.

Introduction

Prolactin (PRL) is a polypeptide hormone predominantly secreted by lactotrophs of the anterior pituitary. Beyond reproduction and lactation, PRL is involved in a broad spectrum of functions, including metabolism control, behavior, immunoregulation, osmoregulation and neuroendocrine response to stress (1). It has been accepted that lactotrophs have high basal secretory activity and that the main control of PRL secretion is exerted by hypothalamic inhibition.. In fact, the lack of a specific endocrine gland as its target and the multiplicity of PRL actions result in the absence of a classical negative feedback control (2).

A significant body of evidence shows that dopamine (DA) is the most important hypothalamic prolactin-inhibiting factor (3). This catecholamine exerts a direct effect on lactotrophs through binding to dopaminergic D2 receptor subtype expressed on their cell membrane. Activation of this receptor results in the suppression of PRL gene expression, inhibition of PRL exocytosis, reduction of lactotroph proliferation and induction of apoptosis (3-5).

Due to the lack of a classical hormone-mediated negative feedback pathway, PRL itself provides the afferent signal necessary to promote such a regulatory mechanism in a process known as short-loop feedback. Through the expression of PRL receptors (PRLR) in dopaminergic neurons, PRL stimulates hypothalamic DA synthesis and increases the release of DA in the pituitary portal blood (6). Therefore, additional PRL secretion from lactotrophs is suppressed. In addition, we observed that PRL exerts control actions at pituitary level itself, increasing apoptosis and reducing proliferation of lactotrophs (7).

Dopamine neurons that control PRL secretion are located in the hypothalamic arcuate and periventricular nuclei. These neurons are arranged into three sub-populations: the tuberoinfundibular (TIDA), tuberohypophyseal (THDA), and periventricular hypophyseal (PHDA) dopaminergic systems (1). TIDA neurons originate in the arcuate

nucleus and project to the median eminence, releasing DA into the pituitary long portal system. While THDA neurons project from the arcuate nucleus to the pituitary neurointermediate lobe PHDA neurons originate in the periventricular nucleus and end in the intermediate lobe. THDA and PHDA neurons transport DA to the anterior pituitary through short portal vessels from the neurointermediate lobe (6).

Dopamine is synthesized from the amino acid tyrosine by two enzymes that act sequentially. Tyrosine hydroxylase (TH), the rate-limiting enzyme, converts this amino acid to L-Dopa. Then, L-Dopa is decarboxylated to DA by aromatic L-amino acid decarboxylase (AADC). The synthesized DA is stored at high concentration inside secretory vesicles. Such structures prevent DA molecules from enzymatic degradation, minimize its diffusion through the cytoplasmic membrane, regulate its secretion by exocytosis, and enable its rapid cellular replenishment. Dopamine is translocated from the cytoplasm into the secretory vesicles by the vesicular monoamine transporter (VMAT). Transport of DA to vesicles is mediated by an electrochemical gradient generated by an ATP-dependent H⁺ pump. Two isoforms of this vesicular transporter coexists: VMAT1 and VMAT2. They arise from distinct but related genes that encode proteins of ~520 residues (8). VMAT1 is present in developing neurons, peripheral tissues, and in some endocrine cells. VMAT2 is expressed in all major monoaminergic neurons throughout the brain (3).

Dopamine can also undergo oxidative deamination by monoamine oxidase (MAO) to produce dihydroxyphenylacetic acid (DOPAC) and reactive oxygen species (ROS) (9).

In addition to dopaminergic neurons expressing TH and AADC, there are monoenzymatic ones that express only one of the enzymes of DA synthesis. In fact, the arcuate nucleus of the hypothalamus is rich in monoenzymatic neurons. Numerous monoenzymatic TH axons terminate in the median eminence, close to the primary capillary of the hypophyseal portal system (10). These observations suggest a pathway for the delivery of L-Dopa towards the hypophyseal portal circulation. In fact, while it was reported in female rats that the portal plasma DA concentration is around 6 ng/ml (11), Telford *et al.* (1992) have observed that the L-Dopa concentration is around 40 ng/ml in NSD 1015-treated animals (12).

The synthesis of DA by anterior pituitary cells has long been in debate. Previous research described that in some physiological or experimental conditions the anterior pituitary expresses TH (13) and synthesizes DA (14). However, in other studies TH activity in the anterior pituitary was not detected (12, 15). In fact, Schussler *et al* (1995) reported that TH primary transcript suffers alternative splicing in the anterior pituitary, suggesting that this gland produces TH proteins with no enzymatic activity (16).

On the other hand, the findings about AADC activity in the anterior pituitary are contradictory (17, 18). The expression of TH in the rat anterior pituitary by an adenoviral vector reduces the gland hyperplasia and circulating PRL levels induced by chronic estradiol treatment. These observations suggest that DA is synthesized in the anterior pituitary gland by TH and AADC enzymes, inhibiting lactotroph growth and PRL secretion (19).

In view of this background, we explored the expression and activity of AADC in the anterior pituitary gland and in the pituitary cell lines AtT20 and GH3. In addition, we

explored the expression of the vesicular monoamine transporter VMAT2 in cells of the anterior pituitary. We observed that DA is synthesized in this gland from L-Dopa by AADC. Moreover, this DA can be released contributing to the control of PRL secretion. In addition, L-Dopa could modify anterior pituitary cell renewal.

Materials and Methods

Drugs

Dulbecco's modified Eagle's medium (DMEM), 3,4-dihydroxy-L-phenylalanine (L-Dopa), 3-hydroxybenzylhydrazine dihydrochloride (NSD-1015), pargyline hydrochloride, 5-Bromo-2'-deoxyuridine (BrdU) were purchased from Sigma-Aldrich (Missouri, USA). Cell culture supplements, 0.05% trypsin-EDTA and anti-guinea pig Alexa 555-conjugated antibody were obtained from Invitrogen (California, USA). Fetal calf serum (FCS) and horse serum were provided by Natocor (Córdoba, Argentina). All terminal deoxynucleotidyl transferase-mediated dUTP nick end labelling (TUNEL) reagents were acquired from Roche Molecular Biochemicals (Mannheim, Germany). The antibodies against anterior pituitary hormones were obtained from Dr. Parlow, National Hormone and Peptide Program (California, USA). Rabbit polyclonal anti-AADC (Cat# AB1569), horseradish peroxidase (HRP) conjugated anti-rabbit (Cat# AP132P) and anti-mouse (Cat# AP130P) antibodies were bought from Millipore (California, USA). The specificity of anti-AADC antibody was previously established in rat (20) and mouse (21). Mouse monoclonal anti-vesicular monoamine transporter 2 (VMAT2) was purchased from Santa Cruz Biotechnology (Cat# Sc-374079, Texas, USA). Anti-rabbit (Cat# FI-1000) and anti-mouse (Cat# FI-2001) FITC-conjugated secondary antibodies were acquired from Vector Laboratories (California, USA). The origin of other materials is indicated below.

Animals

All experimental procedures involving animals were approved by the Animal Care and Use Committee (CICUAL) of the School of Medicine, University of Buenos Aires (approval ID: Res. (CD) N° 2369/2017). Adult male Wistar rats (300-350 g) were housed in groups of five animals per cage in a standard animal facility under controlled conditions of light (12:12 h light-dark cycles) and temperature (22-25 °C). Rats were fed with balanced food pellets and tap water ad libitum. In all cases, animals were sacrificed by decapitation. Parietal bone was broken at the sagittal, coronal and lambdoid sutures and detached using a bone nipper. Brain was gently removed from the cranial cavity using a dental explorer exposing the pituitary gland. Posterior lobe together with the intermediate lobe were detached from the anterior lobe using a tissue forceps. Anterior pituitary was immediately extracted for use.

Primary culture of anterior pituitary cells

Pools of anterior pituitaries from 2 to 3 adult male Wistar rats were cut into small fragments. Sliced fragments were dispersed enzymatically by successive incubations in

DMEM-0.1% BSA (Sigma-Aldrich, Cat# A9418) containing 0.75% trypsin (Invitrogen Cat# 15090046), 10% FCS previously treated with 0.025 % dextran (Sigma-Aldrich Cat# D4751)-0.25 % charcoal (Sigma-Aldrich, Cat# C-5260) (FCS-DC) to remove steroids, and 45 U/ μ L deoxyribonuclease type I (Invitrogen, Cat# 18047-019). Cells were dispersed by extrusion through a Pasteur pipette in Krebs buffer $\text{Ca}^{2+}/\text{Mg}^{2+}$ free. Viability was assessed by trypan blue (Invitrogen, Cat# 15250061) exclusion. Dispersed cells were resuspended in DMEM – 10% FCS-DC and seeded on cover slides in 24-wells tissue culture plates (2×10^5 cells/mL/well). Cultures were kept at 37 °C in a humidified atmosphere containing 5% carbon dioxide. After 24 h, cells were fixed in 4% paraformaldehyde (PFA) and processed for immunofluorescence.

Cell lines culture

AtT20: This mouse ACTH-secreting pituitary adenoma cell line was chosen to carry out our research because they are of pituitary origin and can modulate the release of ACTH upon stimulation with CRH. AtT20 cells are widely used for assessing the effects of different stimulus on cell renewal, viability and ACTH secretion (22-28). These cells lack functional D2 receptors (29, 30). The cells were cultured in 75 cm² tissue flasks without additional surface treatment, containing DMEM medium supplemented with 2 mM L-glutamine, 0.1 mg/mL Gentamicin, and 10% FCS-DC.

GH3: This somatotroph cell line is derived from a pituitary tumor of a female rat. Although these cells lack functional D2 receptor (31), they are often used in studies on rat pituitary cell function as it has been reported that these cells secrete PRL (32). The cells were cultured in 100 mm diameter Petri's dishes without additional surface treatment, containing DMEM medium supplemented with 20 μ L/mL MEM amino acids, 2 mM L-glutamine, 0.1 mg/mL Gentamicin, and 10% FCS-DC.

PC12: We selected this rat pheochromocytoma cell line as a positive control for our experiments based on its dopaminergic properties which resemble DA neurons (33, 34). Cells were undifferentiated since enzyme expression and DA content are higher than NGF-treated cells (34). PC12 cells were cultured in 100 mm diameter Petri's dishes without additional surface treatment, containing DMEM medium supplemented with 0.1 mg/mL Gentamicin, 10% FCS-DC, and 5% horse serum.

All cell lines were cultured in monolayer to a confluence of 80%. Cells were replicated once every three days during the logarithmic phase of growth up to the 7th passage. Cultures were kept at 37 °C in a humidified atmosphere containing 5% carbon dioxide.

Immunofluorescence

In order to identify the populations of anterior pituitary cells expressing AADC or VMAT2, we performed double indirect immunofluorescence staining. Cover slides containing 4% PFA fixed cells from anterior pituitary cell primary culture were permeabilized with 10 mM sodium citrate buffer (pH 6.0) using a microwave oven at 100 mm diameter Petri's dishes with flat and standard-treated surface 350 watts (AADC) or 700 watts (VMAT2) for 5 min. AADC cover slides were additionally permeabilized with PBS-0.5% Triton X-100. Non-specific sites were blocked with either 5% inactivated goat serum (Sigma) or 5% inactivated horse serum in PBS-0.5%

Triton for 1 h. After blockage, cells were incubated for 1 h with anti-ACTH (1/3000), anti-PRL (1/3000), anti-GH (1/1500), or anti-LH (1/500) antibodies. Cells were incubated overnight at 4°C with an anti-AADC (1/25) or an anti-VMAT2 (1/20) antibody, washed and incubated with FITC-conjugated anti-rabbit (1/100), or anti-mouse (1/100) and Alexa 555-conjugated anti-guinea pig antibodies (1/100) for 1 h. Non-specific control was either incubated with inactivated serum or the IgG subtype instead of primary antibody. Finally, cover slides were mounted with Vectashield containing 4',6-diamidino-2-phenylindole (DAPI) for DNA staining (Vector Laboratories, CA, USA) and visualized in an Axio Scope A1 fluorescence light microscope (Carl Zeiss; Jena, Germany) coupled to a digital camera (DP73, Olympus; Tokyo, Japan).

The expression of AADC and VMAT2 was also evaluated in AtT20 and GH3 cells. Cells were harvested with 0.05% trypsin-EDTA (2 min at 37 °C) and seeded on cover slides in 24-well tissue culture plates (2×10^5 cells/ml/well). Cells were processed as described above. PC12 cells were used as positive control for AADC and VMAT2 expression.

Western Blot

Total proteins were extracted from anterior pituitary glands and striatum from adult male Wistar rats, AtT20, GH3, and PC12 cells with lysis buffer (pH 7.4) containing 10 mM Tris, 150 mM NaCl, 2 mM EGTA, 1% Triton X-100, 2.5 mM NaF, 0.5 mM Na_3VO_4 , and a protease inhibitor cocktail (1/100; Sigma, Cat# P8340). Following homogenization and centrifugation at 16,000 g for 40 min, the supernatant was used for the immunoblot assay. The protein content of each sample was determined by the Bradford protein assay (BioRad Laboratories; California, USA). Thirty μg of total proteins were size-fractionated in 12% SDS-polyacrylamide gel and electrotransferred (66 mA, overnight) to PVDF membranes (BioRad, Cat# 162-0177). Correct protein loading and transfer efficiency were assessed by membrane staining with red Ponceau. Then, blots were blocked for 2 h in 5% non-fat dry milk PBS 0.1% Tween 20 (PBST) and incubated overnight at 4°C with anti-AADC (1/400), or anti-VMAT2 (1/100) antibodies in blocking buffer. After washing, membranes were incubated 1 h with HRP-conjugated anti-rabbit or anti-mouse antibody (1/1000) in blocking buffer. Immunoreactivity was detected by enhanced chemiluminescence (Kalium technologies, Argentina) in a G Box Chemi HR16 imaging system (Syngene; Cambridge, UK).

Determination of DA and DOPAC levels

In anterior pituitary experiments, the concentration of tissue and secreted DA and DOPAC were determined by high-performance liquid chromatography (HPLC) using a Spectra System P2000 equipment coupled to an electrochemical detector (BAS CC-5). Tissue samples were lysed and deproteinized in 0.2 N HClO_4 . Homogenates and culture media samples were centrifuged at 11,500 g for 2 min. The supernatant (20 μL) was injected into a 3.9 x 15 cm Nova-Pak C18 (Waters; Massachusetts, USA) reverse phase column. The mobile phase used for the separation consisted of 0.076 M $\text{NaH}_2\text{PO}_4 \cdot \text{H}_2\text{O}$, 0.99 mM EDTA, PicB8 (WAT085142, Waters) 4.8 mL/L, and 7% methanol. The

electrode potential was fixed at 0.7 V and the detector sensitivity was set to 2 for better peak resolution on chromatograms. Peak heights were measured by Peak Simple Chromatography Data System (Model 302 Six Channel 181 USB). Values were quantified based on standard curves using the same software. Dopamine and DOPAC contents per sample were expressed as pmol/mg of tissue. Assay sensitivities were 0.122 pmol for DA and 0.883 pmol for DOPAC.

The intracellular content of DA and DOPAC in AtT20 and GH3 cells was measured by HPLC as described above. Cells were seeded on 24-wells tissue culture plates (3×10^5 cells/ml/well) and kept in culture for 48 h. Afterwards, cells were incubated with or without an AADC inhibitor (NSD-1015, 10 μ M) or a MAO inhibitor (pargyline, 10 μ M) for 30 min. Then, L-Dopa (1 or 10 μ M) was added for further 2 h. DA and DOPAC content per sample was normalized to total protein content (pmol/ μ g of protein).

Prolactin and DA release experiments

Anterior pituitaries from adult male rats were cut into two halves and stabilized for 30 min in DMEM containing 0.1% BSA and 500 μ M ascorbic acid at 37 °C. After this period, the fragments were treated with or without L-DOPA (10 μ M, 2 h). Dopamine and PRL release was measured in conditioned media. Dopamine and DOPAC content was evaluated by HPLC as described above. The levels of PRL in each sample were determined by an ultrasensitive ELISA developed by Guillou *et al.* (35). PRL content per sample was expressed as ng/mg tissue.

ACTH release experiments

AtT20 cells were seeded on 24-well tissue culture plates (2.5×10^5 cells/ml/well) and kept in culture for 48 h. After this period, cells were preincubated in the presence or absence of NSD-1015 (1 μ M) for 30 min and, then, treated with or without L-Dopa (1 μ M, 3 h). All groups were incubated either under basal or CRH-stimulated (100 nM, 3 h) (Bachem, California, USA) conditions. Next, media were collected and centrifuged. ACTH media content was assayed using a rat/mouse EIA kit (EK-001-21; Phoenix Pharmaceuticals Inc., California, USA) following the manufacturer's instructions. ACTH content per sample was expressed as ng/mL.

Apoptosis and proliferation experiments

AtT20 cells were seeded on cover slides in 24-wells tissue culture plates (10^5 cells/ml/well) for TUNEL or BrdU incorporation assays and kept in culture for 48 h. Later, cells were incubated with or without L-Dopa (1 μ M; 8 h) in the presence or absence of NSD-1015 (1 μ M) or MAO inhibitor pargyline (10 μ M). Inhibitors were added 30 min before L-Dopa. For the proliferation assay, BrdU (200 μ M, 8 h) was added to the culture media. After incubation periods, cells were fixed as previously described for immunofluorescence.

For the BrdU incorporation assay, cells were permeabilized with 10 mM sodium citrate buffer (pH 6.0) using a microwave oven at 350 watts for 5 min (90°C). Next, cover slides were incubated for 1 h with DNase (Invitrogen, Cat#18047-019) (100 UI/ml) at

37 °C. Then, cells were blocked with 10% horse serum in PBS-0.2% Triton for 1 h and incubated overnight at 4 °C with an anti-BrdU antibody (1/200, BD Bioscience Cat# 555627; New Jersey, USA). Cells were washed and incubated with a FITC-conjugated anti-mouse antibody (1/100). Cover slides were mounted with Vectashield containing DAPI and visualized in a fluorescent light microscope. Non-specific control cover slides were incubated without BrdU. The percentage of proliferative cells was calculated as [BrdU⁺ cells/total cells] x 100.

For the TUNEL assay, after permeabilization, DNA strand breaks were labelled with digoxigenin-dUTP (1/250) using terminal deoxynucleotidyl transferase (25 U/μL). After incubation with 10% sheep serum (Sigma) in PBS-2% BSA for 1 h, cells were incubated with a FITC-conjugated anti-digoxigenin antibody (1/10) for 1 h to detect incorporation of nucleotides into the 3'-OH end of damaged DNA. Cover slides were mounted with Vectashield containing DAPI and visualized in a fluorescent light microscope. Non-specific control slides were incubated without terminal deoxynucleotidyl transferase. The percentage of apoptotic cells was calculated as [TUNEL⁺ cells/total cells] x 100.

Cells were counted using the multi-point option of ImageJ software (1.50e, Wayne Rasband, National Institutes of Health, USA).

Statistical analysis

GraphPad Prism version 6.00 for Windows (GraphPad Software, California, USA) was used for statistical data analysis.

DA and DOPAC content experiments: All data are presented as mean ± SEM. Statistical analysis was performed using two-tailed unpaired t-test or one way ANOVA followed by Tukey's multiple comparisons test. Differences were considered significant if p<0.05.

PRL release experiments: Results are shown as mean ± SEM. Statistical analysis was performed using a two-tailed unpaired t-test. Differences were considered significant if p<0.05.

ACTH release experiments: Results are displayed as mean ± SEM. Two-way ANOVA followed by Newman-Keuls' multiple comparisons test was used to analyze the data. Differences were considered significant if p<0.05.

Apoptosis and proliferation experiments: Data are expressed as the percentage of BrdU or TUNEL-positive cells ± 95% confidence limits (CL) of the total number of cells (evaluated by DAPI nuclear staining) counted in each specific condition. Differences between proportions were analyzed by the χ^2 test and were considered significant if p<0.05.

Results

AADC and VMAT2 expression in the anterior pituitary gland

In order to study whether the anterior pituitary can decarboxylate L-Dopa to DA, we explored the expression of AADC in this gland by western blot. Figure 1A shows a

single band at 55 kDa corresponding to AADC (36). To determine the cell types within the anterior pituitary that express AADC, double immunofluorescence for this enzyme and four anterior pituitary hormones was performed. As shown in Figure 1B, AADC was localized in corticotrophs, lactotrophs, somatotrophs and gonadotrophs.

We also studied the expression of VMAT2 in the anterior lobe to determine whether DA could be stored in this gland. By means of western blot, we showed VMAT2 expression (single band at 63 kDa) in the anterior pituitary (Fig. 2A). Immunofluorescence revealed that the vesicular transporter is also expressed in all pituitary cell subpopulations studied (Fig. 2B).

Dopamine synthesis by the anterior pituitary gland

Since AADC is expressed in cells of the anterior lobe, we studied the activity of this enzyme in anterior pituitaries incubated with L-Dopa ex vivo. We observed that the content of DA (Fig. 3A) and DOPAC (Fig. 3B) increased in the presence of L-Dopa (10 μ M), indicating sequential AADC and MAO activities in this gland.

The presence of VMAT2 in the anterior lobe suggests the existence of DA-containing vesicles. Thus, we evaluated whether DA could be secreted from the anterior pituitary. We observed that L-Dopa increased DA content in incubation media (Fig. 3C) indicating that DA synthesized from L-Dopa by AADC is released from anterior pituitary cells.

In order to assess whether DA produced from L-Dopa regulates PRL secretion, we measured PRL content in culture media from tissues incubated with L-Dopa. The presence of L-Dopa decreased PRL concentration in the media (Fig. 3D), suggesting that the anterior pituitary could regulate PRL secretion through an auto/paracrine mechanism mediated by endogenously produced DA.

Dopamine synthesis by anterior pituitary cell lines

Next, we determined AADC and VMAT2 expression in GH3 and AtT20 cells by western blot and immunofluorescence. The PC12 cell line was used as a positive control. Both GH3 and AtT20 cells expressed AADC and VMAT2 (Fig. 4).

To evaluate the activity of AADC in these cell lines, we determined the synthesis of DA from L-Dopa by HPLC. Although we did not detect AADC activity in GH3 cells (data not shown), AtT20 cells incubated with L-Dopa (1 and 10 μ M) produced DA and DOPAC, an effect abolished by the AADC inhibitor NSD-1015 (10 μ M) (Fig. 5A, B). Additionally, the presence of MAO inhibitor pargyline (10 μ M) increased DA content in response to L-Dopa (10 μ M) and prevented the production of DOPAC (Fig. 5C). These results indicate that AtT20 cells metabolize L-Dopa to DA by AADC and that DA is oxidized to DOPAC by MAO.

Effects of L-Dopa on ACTH release from AtT20 cells

Considering that AADC activity was detected in AtT20 cells, we studied whether the conversion of L-Dopa to DA or L-Dopa per se could alter ACTH secretion. AtT20 cells were incubated with L-Dopa (1 μ M) with or without NSD-1015 (1 μ M). In the absence of NSD-1015, with an active AADC, L-Dopa did not affect basal or CRH-stimulated

ACTH secretion (Fig. 6A, B). However, the co-treatment with L-Dopa and NSD-1015 reduced ACTH secretion under CRH-stimulated conditions (Fig. 6B). These data suggest that L-Dopa per se could act on stimulated ACTH secretion, independently of its conversion to DA.

Effects of L-Dopa on apoptosis and proliferation of AtT20 cells

We then investigated the effects of the co-treatment with L-Dopa and NSD-1015 on cell renewal in the AtT20 cell line. These cells were incubated with L-Dopa (1 μ M) in the presence or absence of NSD-1015 (1 μ M). While L-Dopa increased the percentage of apoptotic cells, the presence of NSD-1015 and L-Dopa induced a reduction in apoptotic cell number (Fig. 7A). On the contrary, L-Dopa reduced the percentage of proliferative AtT20 cells but, when its conversion to DA was inhibited by NSD-1015, L-Dopa enhanced their proliferation rate (Fig. 7B). NSD-1015 per se did not affect apoptosis or proliferation (Fig. 7A, B). Thus, DA synthesized from L-Dopa exerts a proapoptotic and antiproliferative action. In contrast, L-Dopa per se induces antiapoptotic and proliferative effects in AtT20 cells.

Effects of MAO inhibition on apoptosis and proliferation of AtT20 cells

Dopamine can trigger apoptosis in the anterior pituitary through D2R-dependent or -independent mechanisms (4, 5, 37). Previous studies reported the absence of D2R expression in AtT20 cells (30). Therefore, the observed effects of DA on proliferation and apoptosis in these cells may result from D2R independent signaling. Hence, we hypothesized that the oxidation of DA by MAO, which produces DOPAC and ROS, could be involved in the effects of DA in AtT20 cells. To prevent DA oxidative metabolism, AtT20 cells were co-incubated with L-Dopa (1 μ M) and the MAO inhibitor pargyline (10 μ M). The inhibition of MAO activity prevented the increase in apoptosis and the reduction in proliferation rates induced by L-Dopa (Fig. 8A, B). These results indicate that the proapoptotic and antiproliferative actions of DA produced from L-Dopa in AtT20 cells depend on MAO activity.

Discussion

In this study we demonstrated that anterior pituitary cells synthesize DA from L-Dopa and this DA can act in an autocrine or paracrine fashion to inhibit PRL secretion. In addition, in corticotroph-like cells, we observed effects produced not only by DA derived from L-Dopa but also by L-Dopa per se, suggesting that this precursor can affect anterior pituitary physiology in a direct manner.

The synthesis of DA by the anterior pituitary has been extensively discussed (13, 14). However, it was observed that this gland did not express a functional TH under physiological conditions (11, 20). Few works suggested the presence of AADC in the pituitary gland through indirect evidence. For example, the expression of TH in the anterior pituitary induced by an adenoviral vector reduces hyperplasia and circulating

PRL levels elicited by chronic estradiol treatment. These effects were attributed to DA produced in this gland, suggesting the presence of functional AADC (19).

Herein, we provide direct evidence of AADC immunoreactivity in the anterior pituitary gland. Since the anterior lobe is mainly integrated by hormone-producing cells, we detected AADC in these cell types including corticotrophs and lactotrophs. Although it has been suggested that the anterior pituitary cannot decarboxylate L-Dopa to DA (18), we demonstrated in vitro that the anterior lobe could synthesize DA in the presence of L-Dopa. Furthermore, we detected the oxidative metabolite DOPAC which is increased with the addition of L-Dopa. These results agree with previous assays reporting MAO activity in the anterior pituitary (15, 38).

The potential regulatory role of L-Dopa in the anterior pituitary might implicate the secretion of endogenous DA from this lobe. We showed the expression of VMAT2 in the anterior pituitary, suggesting that this lobe could store and eventually secrete the locally produced DA. In fact, we detected an increase in DA released to the incubation media from tissues previously incubated in the presence of L-Dopa.

To further support our findings of AADC activity, we studied the inhibitory effect of DA on the secretion of PRL in vitro. Prolactin levels were measured in conditioned media from anterior pituitaries incubated in the presence or absence of L-Dopa. Treatment with L-Dopa is known to suppress PRL circulating levels in laboratory animals (39-43) and in Parkinson's (44, 45) or non-parkinsonian patients (46, 47). These in vivo effects could be produced at hypothalamic and/or anterior pituitary levels. In our study we observed that L-Dopa decreased in vitro PRL release from incubated anterior pituitaries, suggesting that these reported effects are mediated, at least partially, by anterior pituitary-synthesized DA. Our findings, together with early reports showing AADC activity in the anterior pituitary (15, 48), indicate that this lobe can produce autocrine/paracrine signals which may involve DA suggesting a potential role of L-Dopa metabolism in the physiology of this gland.

In the mediobasal hypothalamus, which includes the median eminence, the presence of monoenzymatic neurons expressing TH or AADC has been demonstrated (49) suggesting that L-Dopa can be released from TH expressing neurons to AADC expressing ones for DA synthesis. Moreover, it has been proposed that L-Dopa can be released by TH expressing neurons to the portal vessels reaching the anterior pituitary gland (10). In fact, Telford *et al.* have shown that the concentration of L-Dopa is higher in portal blood than in peripheral circulation. The authors conclude that the major source of L-Dopa in the anterior pituitary is the portal blood supply because L-Dopa was not detected in this lobe when the portal circulation was interrupted by separating the pituitary stalk (12). Based on reported concentrations in portal blood of DA (6 ng/ml in diestrus rats; (11)) and L-Dopa (40 ng/ml in female rats treated with NSD 1015; (12)), we could assume that the greatest contribution of DA would be from an endogenous (anterior pituitary) source. However, the concentration of L-Dopa in the portal circulation was measured in rats treated with NSD 1015 (an AADC inhibitor), which could overestimate the amount of L-Dopa reaching the anterior pituitary under physiological conditions.

There are other tissues that produce DA from L-Dopa. For example, kidney proximal tubules synthesize DA from circulating L-Dopa, which is then converted to DA by AADC (50). In summary, we demonstrated for the first time that DA is synthesized from L-Dopa in the anterior pituitary gland and that this locally produced DA inhibits anterior pituitary PRL secretion.

Given the small number of corticotrophs in the anterior pituitary gland, we used the AtT20 cell line to achieve part of our goals. This tumor-derived cell line allowed us to study the direct actions of L-Dopa on ACTH secretion and cell turnover as a first experimental approach. Nonetheless, some caution should be taken when interpreting the results obtained.

Horellou *et al.* suggested the presence of AADC in AtT20 cells since they detected intracellular and secreted DA after transducing cells with TH cDNA (51). In line with this, we showed that AtT20 cells expressed AADC and VMAT2, and the intracellular content of DA increased after incubation with L-Dopa. In addition, AADC blockade made DA levels undetectable, indicating that the enzyme is responsible for the production of this catecholamine. We hypothesized oxidative deamination might represent one of the mechanisms for DA inactivation within corticotrophs. To explore this, we studied the production of DOPAC by MAO in AtT20 cells. The accumulation of DOPAC increased in an L-Dopa concentration-dependent manner, and the inhibition of MAO with pargyline abolished DOPAC synthesis.

Most in vitro studies investigated the effects of high concentrations of L-Dopa (50 μ M-1 mM) for extended periods (from 12 h to several days) (52). In our study, the concentrations of L-Dopa tested in the experiments were 1 and 10 μ M. These selected concentrations are comparable to the levels found in the plasma of portal vessels (12).

To elucidate whether L-Dopa treatment alters the secretion of ACTH, we examined the effects of locally produced DA and AADC inhibition on basal and CRH-stimulated secretion of ACTH. Inhibition of AADC by NSD-1015 in AtT20 cells showed that L-Dopa decreased ACTH secretion under stimulated conditions. To the best of our knowledge, we provide the first evidence showing direct effects of L-Dopa on the secretory function of AtT20 cells. In contrast to other reports demonstrating a D2R-dependent dopaminergic inhibition of ACTH secretion (53), we did not observe such effect of local DA in either condition, perhaps due to the lack of D2R expression in AtT20 cells (30). The reduction in CRH-stimulated ACTH release in the presence of AADC inhibitor suggests that L-Dopa per se interferes with this stimulatory signal. These data are consistent with L-Dopa potential role as a neurotransmitter or neuromodulator (54). According to Misu *et al.*, the existence of neurons that contain L-Dopa as an end-product and the fact that other by-products of its metabolism do not mimic L-Dopa responses in the presence of AADC inhibition, suggest that this precursor fits the criteria to be accepted as an extracellular messenger (54). In fact, L-Dopa was reported to have binding activity for the gene product of *ocular albinism 1* (OA1), GPR143, a G protein-coupled receptor (GPCR). Moreover, L-Dopa induced intracellular Ca²⁺ response in cell lines that express GPR143 (55). While GPR143 is expressed in the central and peripheral nervous system, its expression in the anterior pituitary has not been explored yet.

Although the conclusions that can be drawn from the experiments carried out with cell lines are limited, our results suggest that corticotrophs could exert a paracrine function producing DA and contributing in this way to the inhibition of PRL secretion.

The role of L-Dopa in apoptosis and survival of dopaminergic neurons has been widely studied (55-61), but such effects remain unexplored in corticotrophs. Based on this premise, we investigated the effect of L-Dopa in apoptosis and proliferation of AtT20 cells. In agreement with early reports describing the suppression of lymphocyte proliferation by L-Dopa (62, 63), we observed that this precursor, when converted to DA, is apoptotic and anti-proliferative in AtT20 cells. On the contrary, when AADC was inhibited, L-Dopa acted as an anti-apoptotic and proliferative factor, as described for other cell types (64, 65). Our findings provide evidence that the cytotoxicity of L-Dopa can be attributed, at least in part, to the formation of DA within the cells. On the other hand, AADC inhibition unmasked a protective role of L-Dopa in the renewal of corticotrophs. This last result highlights this agent would exert direct effects on cell viability without the requirement of its metabolism by AADC (52, 66, 67). Even though we observed that L-Dopa per se decreases short-term ACTH secretion, we cannot rule out that chronic administration may induce other effects on ACTH release, due to the proliferative actions of L-Dopa in corticotrophs. More studies are required to clarify this point.

Further experiments were conducted to examine the mechanism by which DA synthesized from L-Dopa may be cytotoxic to AtT20 cells. Since our cells do not express D2R, we hypothesized that DA might be triggering its apoptotic and anti-proliferative effects by D2R-independent mechanisms (68, 69). It is known that DA can oxidatively damage cells through its metabolism by MAO (36). As we observed DOPAC production within AtT20 cells, the actions of the oxidative metabolism of endogenous DA on cell turnover were evaluated. Dopamine apoptotic and anti-proliferative actions were not observed when MAO was inhibited, indicating that the activity of this enzyme is essential to observe DA effects on apoptosis and proliferation of corticotroph cells.

In conclusion, L-Dopa is metabolized by AADC to form DA and oxidized by MAO to produce DOPAC in the anterior pituitary. Also, this local DA is released as a paracrine messenger modulating the secretion of PRL. On the other hand, L-Dopa per se alters the secretion of ACTH from AtT20 cells by modifying the action of CRH. Additionally, it decreases apoptosis and increases proliferation rates in this cell line. In addition to its potential physiological role, L-Dopa treatment is the gold standard for Parkinson's disease treatment (70). In view of our results, it is relevant to study the functions of the pituitary gland in parkinsonian patients treated with L-Dopa and AADC inhibitors.

Acknowledgement

We would like to thank Dr Carlos Davio for the opportunity to work at the Instituto de Investigaciones Farmacológicas. We would also like to thank Dr Cora Cymeryng from the Centro de Estudios Farmacológicos y Botánicos for the kind donation of AtT20 cells.

Disclosure Statement

The authors have no conflicts of interest to declare.

Funding Sources

This project was supported by grants from CONICET (PIP-0772), National Ministry of Science and Technology (PICT 2013-1900) and University of Buenos Aires, Argentina.

References

1. Freeman ME, Kanyicska B, Lerant A, Nagy G. Prolactin: structure, function, and regulation of secretion. *Physiol Rev.* 2000;80(4):1523-631.
2. Fitzgerald P, Dinan TG. Prolactin and dopamine: what is the connection? A review article. *J Psychopharmacol.* 2008;22(2 Suppl):12-9.
3. Ben-Jonathan N, Hnasko R. Dopamine as a prolactin (PRL) inhibitor. *Endocr Rev.* 2001;22(6):724-63.
4. Radl DB, Ferraris J, Boti V, Seilicovich A, Sarkar DK, Pisera D. Dopamine-induced apoptosis of lactotropes is mediated by the short isoform of D2 receptor. *PLoS One.* 2011;6(3):e18097. PMID: 3064585.
5. Radl DB, Zarate S, Jaita G, Ferraris J, Zaldivar V, Eijo G, et al. Apoptosis of lactotrophs induced by D2 receptor activation is estrogen dependent. *Neuroendocrinology.* 2008;88(1):43-52.
6. Grattan DR. 60 YEARS OF NEUROENDOCRINOLOGY: The hypothalamo-prolactin axis. *J Endocrinol.* 2015;226(2):T101-22. PMID: 4515538.
7. Ferraris J, Zarate S, Jaita G, Boutillon F, Bernadet M, Auffret J, et al. Prolactin induces apoptosis of lactotropes in female rodents. *PLoS One.* 2014;9(5):e97383. PMID: 4032245.
8. Gasnier B. The loading of neurotransmitters into synaptic vesicles. *Biochimie.* 2000;82(4):327-37.
9. Meiser J, Weindl D, Hiller K. Complexity of dopamine metabolism. *Cell Commun Signal.* 2013;11(1):34. PMID: 3693914.
10. Ugrumov MV. Brain neurons partly expressing dopaminergic phenotype: location, development, functional significance, and regulation. *Adv Pharmacol.* 2013;68:37-91.
11. Gibbs DM, Neill JD. Dopamine levels in hypophysial stalk blood in the rat are sufficient to inhibit prolactin secretion in vivo. *Endocrinology.* 1978;102(6):1895-900.

12. Telford N, May PC, Sinha YN, Porter JC, Finch CE. Dopa accumulates in the hypothalamic-hypophysial portal vessels and is taken into the anterior pituitary of NSD-1015-treated rodents. *Neuroendocrinology*. 1992;55(4):390-5.
13. Jaubert A, Drutel G, Leste-Lasserre T, Ichas F, Bresson-Bepoldin L. Tyrosine hydroxylase and dopamine transporter expression in lactotrophs from postlactating rats: involvement in dopamine-induced apoptosis. *Endocrinology*. 2007;148(6):2698-707.
14. Fernandez-Ruiz JJ, Esquifino AI, Steger RW, Amador AG, Bartke A. Presence of tyrosine-hydroxylase activity in anterior pituitary adenomas and ectopic anterior pituitaries in male rats. *Brain Res*. 1987;421(1-2):65-8.
15. Saavedra JM, Palkovits M, Kizer JS, Brownstein M, Zivin JA. Distribution of biogenic amines and related enzymes in the rat pituitary gland. *J Neurochem*. 1975;25(3):257-60.
16. Schussler N, Boularand S, Li JY, Peillon F, Mallet J, Biguet NF. Multiple tyrosine hydroxylase transcripts and immunoreactive forms in the rat: differential expression in the anterior pituitary and adrenal gland. *J Neurosci Res*. 1995;42(6):846-54.
17. Iturriza FC, Rubio MC, Gomez Dumm CL, Zieher LM. Catecholamine metabolizing enzymes and synthesis of dopamine in normal and grafted pituitary partes distales. *Neuroendocrinology*. 1983;37(5):371-7.
18. Johnston CA, Spinedi E, Negro-Vilar A. Aromatic L-amino acid decarboxylase activity in the rat median eminence, neurointermediate lobe and anterior lobe of the pituitary. Physiological and pharmacological implications for pituitary regulation. *Neuroendocrinology*. 1984;39(1):54-9.
19. Williams JC, Stone D, Smith-Arica JR, Morris ID, Lowenstein PR, Castro MG. Regulated, adenovirus-mediated delivery of tyrosine hydroxylase suppresses growth of estrogen-induced pituitary prolactinomas. *Mol Ther*. 2001;4(6):593-602.
20. Lu J, Zhou TC, Saper CB. Identification of wake-active dopaminergic neurons in the ventral periaqueductal gray matter. *J Neurosci*. 2006;26(1):193-202.
21. King JM, Muthian G, Mackey V, Smith M, Charlton C. L-Dihydroxyphenylalanine modulates the steady-state expression of mouse striatal tyrosine hydroxylase, aromatic L-amino acid decarboxylase, dopamine and its metabolites in an MPTP mouse model of Parkinson's disease. *Life Sci*. 2011;89(17-18):638-43.
22. Gong YY, Liu YY, Yu S, Zhu XN, Cao XP, Xiao HP. Ursolic acid suppresses growth and adrenocorticotrophic hormone secretion in AtT20 cells as a potential agent targeting adrenocorticotrophic hormone-producing pituitary adenoma. *Mol Med Rep*. 2014;9(6):2533-9.

23. Jian F, Chen Y, Ning G, Fu W, Tang H, Chen X, et al. Cold inducible RNA binding protein upregulation in pituitary corticotroph adenoma induces corticotroph cell proliferation via Erk signaling pathway. *Oncotarget*. 2016;7(8):9175-87.
24. Jian FF, Li YF, Chen YF, Jiang H, Chen X, Zheng LL, et al. Inhibition of Ubiquitin-specific Peptidase 8 Suppresses Adrenocorticotrophic Hormone Production and Tumorous Corticotroph Cell Growth in AtT20 Cells. *Chin Med J (Engl)*. 2016;129(17):2102-8.
25. Lim JS, Eom YW, Lee ES, Kwon HJ, Kwon JY, Choi J, et al. Effects of Oxytocin on Cell Proliferation in a Corticotroph Adenoma Cell Line. *Endocrinol Metab (Seoul)*. 2019;34(3):302-13.
26. Liu F, Khawaja X. Basal adrenocorticotropin (ACTH) secretion is negatively modulated by protein phosphatase 5 in mouse pituitary corticotropin AtT20 cells. *Regul Pept*. 2005;127(1-3):191-6.
27. Shida A, Ikeda T, Tani N, Morioka F, Aoki Y, Ikeda K, et al. Cortisol levels after cold exposure are independent of adrenocorticotrophic hormone stimulation. *PLoS One*. 2020;15(2):e0218910.
28. Zhang C, Qiang Q, Jiang Y, Hu L, Ding X, Lu Y, et al. Effects of hypoxia inducible factor-1alpha on apoptotic inhibition and glucocorticoid receptor downregulation by dexamethasone in AtT-20 cells. *BMC Endocr Disord*. 2015;15:24.
29. Wolfe S, Morris S. Dopamine D2 Receptor Isoforms Expressed in AtT20 Cells Differentially Couple to G Proteins to Acutely Inhibit High Voltage-Activated Calcium Channels. *J Neurochem*. 2000;73:2375-82.
30. Wolfe SE, Howard DE, Schetz JA, Cheng CJ, Webber R, Beatty DM, et al. Dopamine D2-receptor isoforms expressed in AtT20 cells inhibit Q-type high-voltage-activated Ca²⁺ channels via a membrane-delimited pathway. *J Neurochem*. 1999;72(2):479-90.
31. Fischberg D, Bancroft C. The D2 receptor: blocked transcription in GH3 cells and cellular pathways employed by D2A to regulate prolactin promoter activity. *Molecular and cellular endocrinology*. 1995;111:129-37.
32. Gershengorn M, Hoffstein S, Rebecchi M, Geras E, Rubin B. Thyrotropin-releasing Hormone Stimulation of Prolactin Release from Clonal Rat Pituitary Cells. *Journal of Clinical Investigation - J Clin Invest*. 1981;67:1769-76.
33. Greene L, Tischler A. Establishment of a Noradrenergic Clonal Line of Rat Adrenal Pheochromocytoma Cells Which Respond to Nerve Growth Factor. *Proc Natl Acad Sci U S A*. 1976;73:2424-8.
34. Enayah S, Vanle B, Fuortes L, Doorn J, Ludewig G. PCB95 and PCB153 change dopamine levels and turn-over in PC12 cells. *Toxicology*. 2017;394.

35. Guillou A, Romano N, Steyn F, Abitbol K, Le Tissier P, Bonnefont X, et al. Assessment of lactotroph axis functionality in mice: longitudinal monitoring of PRL secretion by ultrasensitive-ELISA. *Endocrinology*. 2015;156(5):1924-30.
36. Stansley BJ, Yamamoto BK. L-dopa-induced dopamine synthesis and oxidative stress in serotonergic cells. *Neuropharmacology*. 2013;67:243-51. PMID: 3638241.
37. Jaubert A, Ichas F, Bresson-Bepoldin L. Signaling pathway involved in the proapoptotic effect of dopamine in the GH3 pituitary cell line. *Neuroendocrinology*. 2006;83(2):77-88.
38. Kamberi IA, Kobayashi Y. Monoamine oxidase activity in the hypothalamus and various other brain areas and in some endocrine glands of the rat during the estrus cycle. *J Neurochem*. 1970;17(2):261-8.
39. Kasuya E, Yayou K, Sutoh M. L-DOPA attenuates prolactin secretion in response to isolation stress in Holstein steers. *Anim Sci J*. 2013;84(7):562-8.
40. Prilusky J, Deis RP. Effect of L-dopa on milk ejection and prolactin release in lactating rats. *J Endocrinol*. 1975;67(3):397-401.
41. Richards GE, Holland FJ, Aubert ML, Ganong WF, Kaplan SL, Grumbach MM. Regulation of prolactin and growth hormone secretion. Site and mechanism of action of thyrotropin-releasing hormone, L-dopa and L-5-hydroxytryptophan in unanesthetized dogs. *Neuroendocrinology*. 1980;30(3):139-43.
42. Riegle GD, Meites J. Effects of aging on LH and prolactin after LHRL L-dopa, methyl-dopa, and stress in male rat. *Proc Soc Exp Biol Med*. 1976;151(3):507-11.
43. Watkins BE, McKay DW, Riegle GD. L-Dopa effects on serum LH and prolactin in old and young female rats. *Neuroendocrinology*. 1975;19(4):331-8.
44. Ruggieri S, Falaschi P, Baldassarre M, D'Urso R, De Giorgio G, Rocco A, et al. Prolactin response to acute administration of different L-dopa plus decarboxylase inhibitors in Parkinson's disease. *Neuropsychobiology*. 1982;8(2):102-8.
45. Stypula G, Kunert-Radek J, Stepień H, Zylinska K, Pawlikowski M. Evaluation of interleukins, ACTH, cortisol and prolactin concentrations in the blood of patients with parkinson's disease. *Neuroimmunomodulation*. 1996;3(2-3):131-4.
46. Garcia-Borreguero D, Larrosa O, Granizo JJ, de la Llave Y, Hening WA. Circadian variation in neuroendocrine response to L-dopa in patients with restless legs syndrome. *Sleep*. 2004;27(4):669-73.
47. Saito I, Kawabe H, Hasegawa C, Iwaida Y, Yamakawa H, Saruta T, et al. Effect of L-dopa in young patients with hypertension. *Angiology*. 1991;42(9):691-5.
48. Szabo M, Nakawatase C, Kovathana N, Frohman LA. Effect of the dopa decarboxylase inhibitor MK-486 on L-dopa-induced inhibition of prolactin secretion:

evidence for CNS participation in the L-dopa effects. *Neuroendocrinology*. 1977;24(1):24-34.

49. Melnikova VI, Lyupina YV, Lavrentieva AV, Sapronova AY, Ugrumov MV. Synthesis of dopamine in non-dopaminergic neurons of the mediobasal hypothalamus of adult rats. *Dokl Biol Sci*. 2012;446:286-9.

50. Armando I, Villar VA, Jose PA. Dopamine and renal function and blood pressure regulation. *Compr Physiol*. 2011;1(3):1075-117. PMID: 6342207.

51. Horellou P, Guibert B, Levieil V, Mallet J. Retroviral transfer of a human tyrosine hydroxylase cDNA in various cell lines: regulated release of dopamine in mouse anterior pituitary AtT-20 cells. *Proc Natl Acad Sci U S A*. 1989;86(18):7233-7. PMID: 298031.

52. Lipski J, Nistico R, Berretta N, Guatteo E, Bernardi G, Mercuri NB. L-DOPA: a scapegoat for accelerated neurodegeneration in Parkinson's disease? *Prog Neurobiol*. 2011;94(4):389-407.

53. Olah M, Feher P, Ihm Z, Bacskay I, Kiss T, Freeman ME, et al. Dopamine-regulated adrenocorticotrophic hormone secretion in lactating rats: functional plasticity of melanotropes. *Neuroendocrinology*. 2009;90(4):391-401. PMID: 2826432.

54. Misu Y, Goshima Y, Miyamae T. Is DOPA a neurotransmitter? *Trends Pharmacol Sci*. 2002;23(6):262-8.

55. Goshima Y, Masukawa D, Kasahara Y, Hashimoto T, Aladeokin AC. 1-DOPA and Its Receptor GPR143: Implications for Pathogenesis and Therapy in Parkinson's Disease. *Front Pharmacol*. 2019;10:1119. PMID: 6785630.

56. Liedhegner EA, Steller KM, Mielay JJ. Levodopa activates apoptosis signaling kinase 1 (ASK1) and promotes apoptosis in a neuronal model: implications for the treatment of Parkinson's disease. *Chem Res Toxicol*. 2011;24(10):1644-52. PMID: 3196761.

57. Park KH, Park HJ, Shin KS, Lee MK. Multiple treatments with L-3,4-dihydroxyphenylalanine modulate dopamine biosynthesis and neurotoxicity through the protein kinase A-transient extracellular signal-regulated kinase and exchange protein activation by cyclic AMP-sustained extracellular signal-regulated kinase signaling pathways. *J Neurosci Res*. 2014;92(12):1746-56.

58. Park KH, Shin KS, Zhao TT, Park HJ, Lee KE, Lee MK. L-DOPA modulates cell viability through the ERK-c-Jun system in PC12 and dopaminergic neuronal cells. *Neuropharmacology*. 2016;101:87-97.

59. Shin JY, Park HJ, Ahn YH, Lee PH. Neuroprotective effect of L-dopa on dopaminergic neurons is comparable to pramipexol in MPTP-treated animal model of Parkinson's disease: a direct comparison study. *J Neurochem*. 2009;111(4):1042-50.

60. Stednitz SJ, Freshner B, Shelton S, Shen T, Black D, Gahtan E. Selective toxicity of L-DOPA to dopamine transporter-expressing neurons and locomotor behavior in zebrafish larvae. *Neurotoxicol Teratol.* 2015;52(Pt A):51-6.
61. Zhong SY, Chen YX, Fang M, Zhu XL, Zhao YX, Liu XY. Low-dose levodopa protects nerve cells from oxidative stress and up-regulates expression of pCREB and CD39. *PLoS One.* 2014;9(4):e95387. PMID: 3990701.
62. Josefsson E, Bergquist J, Ekman R, Tarkowski A. Catecholamines are synthesized by mouse lymphocytes and regulate function of these cells by induction of apoptosis. *Immunology.* 1996;88(1):140-6. PMID: 1456449.
63. Slominski A, Goodman-Snitkoff GG. Dopa inhibits induced proliferative activity of murine and human lymphocytes. *Anticancer Res.* 1992;12(3):753-6.
64. Singh AP, Sarkar S, Tripathi M, Rajender S. *Mucuna pruriens* and its major constituent L-DOPA recover spermatogenic loss by combating ROS, loss of mitochondrial membrane potential and apoptosis. *PLoS One.* 2013;8(1):e54655. PMID: 3551850.
65. Xi H, Tao W, Jian Z, Sun X, Gong X, Huang L, et al. Levodopa attenuates cellular apoptosis in steroid-associated necrosis of the femoral head. *Exp Ther Med.* 2017;13(1):69-74. PMID: 5245153.
66. Cheng N, Maeda T, Kume T, Kaneko S, Kochiyama H, Akaike A, et al. Differential neurotoxicity induced by L-DOPA and dopamine in cultured striatal neurons. *Brain Res.* 1996;743(1-2):278-83.
67. Maeda T, Cheng N, Kume T, Kaneko S, Kouchiyama H, Akaike A, et al. L-DOPA neurotoxicity is mediated by glutamate release in cultured rat striatal neurons. *Brain Res.* 1997;771(1):159-62.
68. Al-Azzawi H, Yacqub-Usman K, Richardson A, Hofland LJ, Clayton RN, Farrell WE. Reversal of endogenous dopamine receptor silencing in pituitary cells augments receptor-mediated apoptosis. *Endocrinology.* 2011;152(2):364-73.
69. Rowther FB, Richardson A, Clayton RN, Farrell WE. Bromocriptine and dopamine mediate independent and synergistic apoptotic pathways in pituitary cells. *Neuroendocrinology.* 2010;91(3):256-67.
70. Hornykiewicz O. L-Dopa. *J Parkinsons Dis.* 2017;7(s1):S3-S10. PMID: 5345651.

Figure Legends

Figure 1. AADC is expressed in corticotrophs, lactotrophs, somatotrophs and gonadotrophs. (A) AADC expression in the anterior pituitary was detected by western blot (AP, anterior pituitary; STR, striatum). (B) Primary cultures of anterior pituitary cells from adult male rats were processed for identification of AADC and pituitary hormones by double immunofluorescence. Representative microphotographs show the expression of AADC (green) in PRL, GH, ACTH, and LH positive cells (red). Nuclei were stained with DAPI (blue). Scale bars: 20 μm .

Figure 2. VMAT2 is expressed in corticotrophs, lactotrophs, somatotrophs and gonadotrophs. (A) VMAT2 expression in the anterior pituitary was detected by western blot (AP, anterior pituitary; STR, striatum). (B) Primary cultures of anterior pituitary cells from adult male rats were processed for identification of VMAT2 and pituitary hormones by double immunofluorescence. Representative microphotographs show the expression of VMAT2 (green) in PRL, GH, ACTH, and LH positive cells (red). Nuclei were stained with DAPI (blue). Scale bars: 20 μm .

Figure 3. L-Dopa is metabolized in the anterior pituitary gland and plays a potential role in PRL secretion. Each column represents the mean \pm SEM. (A and B) DA and DOPAC tissue levels (n=7/group) were detected by HPLC in anterior pituitary fragments. In the presence of L-Dopa (10 μM) the content of DA and DOPAC was increased.*p<0.05 (t=2.466 df=11), **p<0.01 (t=3.600 df=11), unpaired t-test. (C) DA was detected by HPLC in conditioned media (n=6 wells/group) from anterior pituitary fragments incubated with or without L-Dopa. In the presence of L-Dopa (10 μM) the content of DA was increased. **p<0.01 (t=4.029; df=10), unpaired t-test (D) PRL content was detected by ELISA in conditioned media (n=14 wells/group) from anterior pituitary fragments incubated with or without L-Dopa (10 μM). **p<0.01 (t=3.875 df=25), unpaired t-test.

Figure 4. AADC and VMAT2 are expressed in anterior pituitary cell lines. GH3 and AtT20 cells were processed for the identification of AADC (A) or VMAT2 (B) by immunofluorescence. Microphotographs show AADC or VMAT2 (green) expression. Nuclei were stained with DAPI (blue). The PC12 cell line was used as a positive control. Results were confirmed by western blot of proteins from GH3, AtT20 and PC12 cells. Scale bars: 20 μm .

Figure 5. DA and DOPAC are produced from exogenous L-Dopa in AtT20 cells. Each column represents the mean \pm SEM (n=4/group). DA (A) and DOPAC (B) were detected in AtT20 cells by HPLC after incubation with 1 or 10 μM L-Dopa. DA and DOPAC were not detectable (ND) in the presence of NSD-1015. **p<0.01 vs. 0 μM L-Dopa, one-way ANOVA (A: F(4,15) = 215.9; B: F(4,15) = 76.19) followed by Tukey's test (C) MAO inhibitor (pargyline, 10 μM) prevents the production of DOPAC and increases the content of DA measured by HPLC. **p<0.01 vs. 10 μM L-Dopa without pargyline, unpaired t-test.

Figure 6. L-Dopa plus an AADC inhibitor reduces CRH-stimulated ACTH secretion from AtT20 cells. Each column represents the mean \pm SEM (n=9 wells/group) of ACTH levels (ng/ml). ACTH was measured in culture media from AtT20 cells by enzyme immunoassay (EIA) both in basal (A) and under CRH (100 nM) stimulated conditions (B). *p<0.05 vs. respective controls without L-Dopa, ^p<0.05 vs. respective control without NSD 1015, two-way ANOVA (A: L-Dopa: F (1, 32) = 1.339, p>0.05; NSD 1015: F (1, 32) = 0.005811; p> 0.05; Interaction: F (1, 32) = 1.276, p>0.05). B: L-Dopa: F(1,31) = 4.749, p<0.05; NSD 1015: F(1,31) = 0.8971, p>0.05; Interaction: F(1,31) = 6.789, p<0.05) followed by Newman-Keuls' multiple comparisons test.

Figure 7. AADC inhibition reverses apoptotic and antiproliferative effects induced by L-Dopa. Each column represents the percentage \pm confidence limit (CL: 95%) of apoptotic (A) or proliferative (B) AtT20 cells (n \geq 1000 cells/group) determined by TUNEL or BrdU incorporation assays, respectively. **p<0.01 vs. respective controls without L-Dopa, ^^p<0.01 vs respective control without NSD-1015, χ^2 test. Lower panels show representative microphotographs of TUNEL+ or BrdU+ cells (green). Nuclei were stained with DAPI (blue). Arrowheads indicate the location of TUNEL or BrdU positive nuclei. Scale bars: 50 μ m.

Figure 8. MAO inhibition reverses apoptotic and antiproliferative effects induced by L-Dopa converted to DA. Each column represents the percentage \pm confidence limit (CL: 95%) of apoptotic (A) or proliferative (B) AtT20 cells (n \geq 1000 cells/group) determined by TUNEL or BrdU incorporation assays, respectively. **p<0.01 vs. respective control without L-Dopa, ^^p<0.01 vs. respective control without pargyline, χ^2 test.

Fig. 1

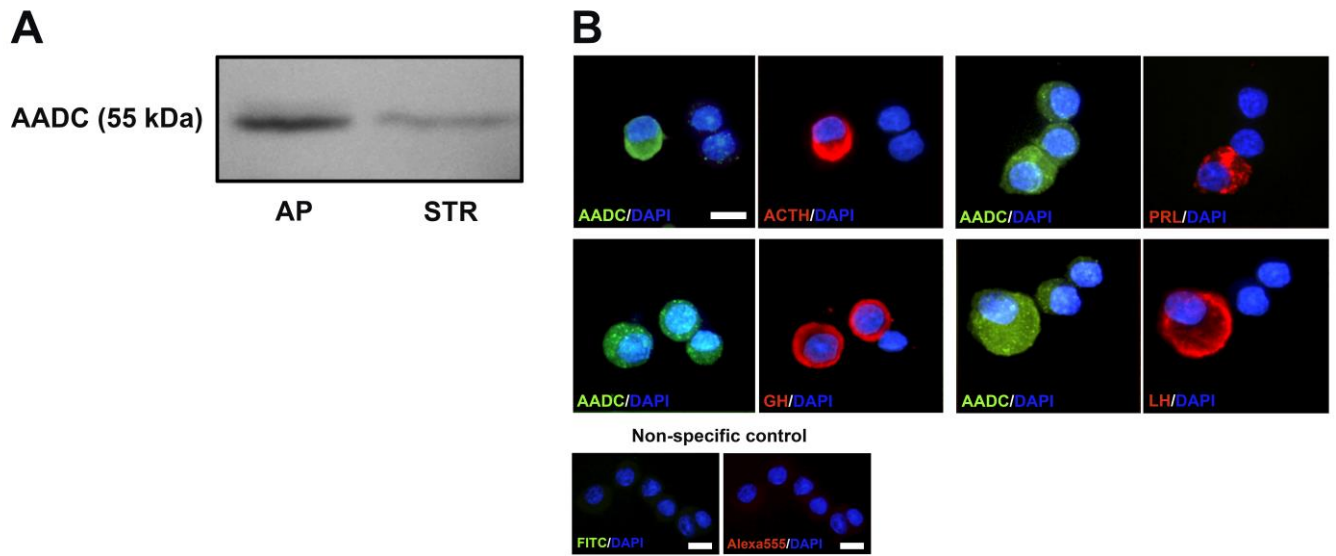


Figure 1. AADC is expressed in corticotrophs, lactotrophs, somatotrophs and gonadotrophs. (A) AADC expression in the anterior pituitary was detected by western blot (AP, anterior pituitary; STR, striatum). (B) Primary cultures of anterior pituitary cells from adult male rats were processed for identification of AADC and pituitary hormones by double immunofluorescence. Representative microphotographs show the expression of AADC (green) in PRL, GH, ACTH, and LH positive cells (red). Nuclei were stained with DAPI (blue). Scale bars: 20 μm.

Fig. 2

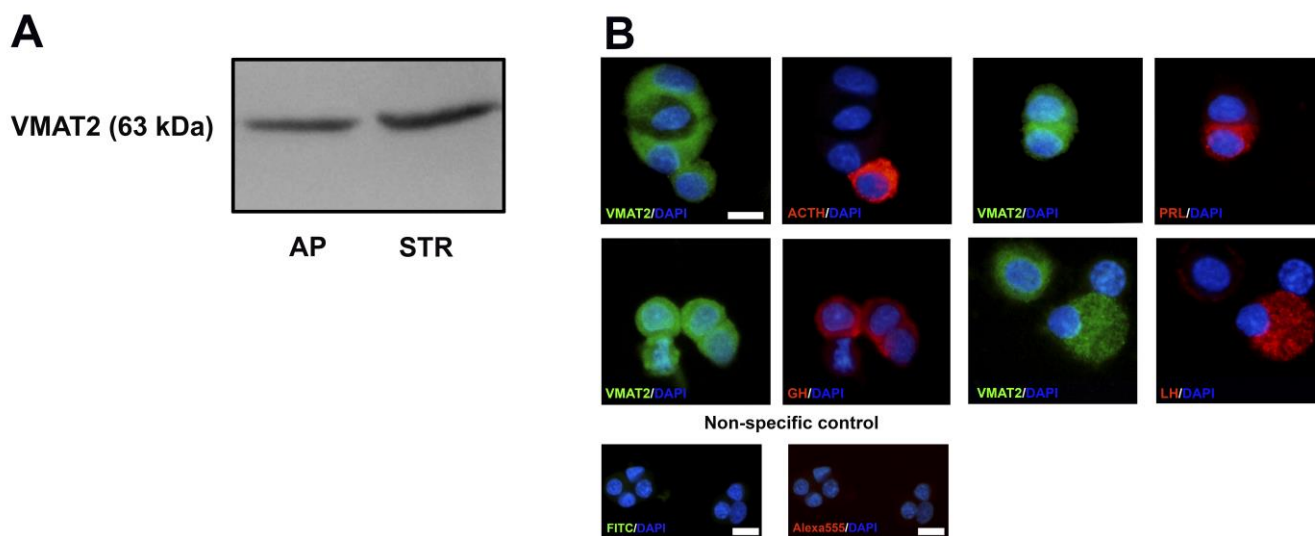


Figure 2. VMAT2 is expressed in corticotrophs, lactotrophs, somatotrophs and gonadotrophs. (A) VMAT2 expression in the anterior pituitary was detected by western blot (AP, anterior pituitary; STR, striatum). (B) Primary cultures of anterior pituitary cells from adult male rats were processed for identification of VMAT2 and pituitary hormones by double immunofluorescence. Representative microphotographs show the expression of VMAT2 (green) in PRL, GH, ACTH, and LH positive cells (red). Nuclei were stained with DAPI (blue). Scale bars: 20 μ m.

Fig. 3

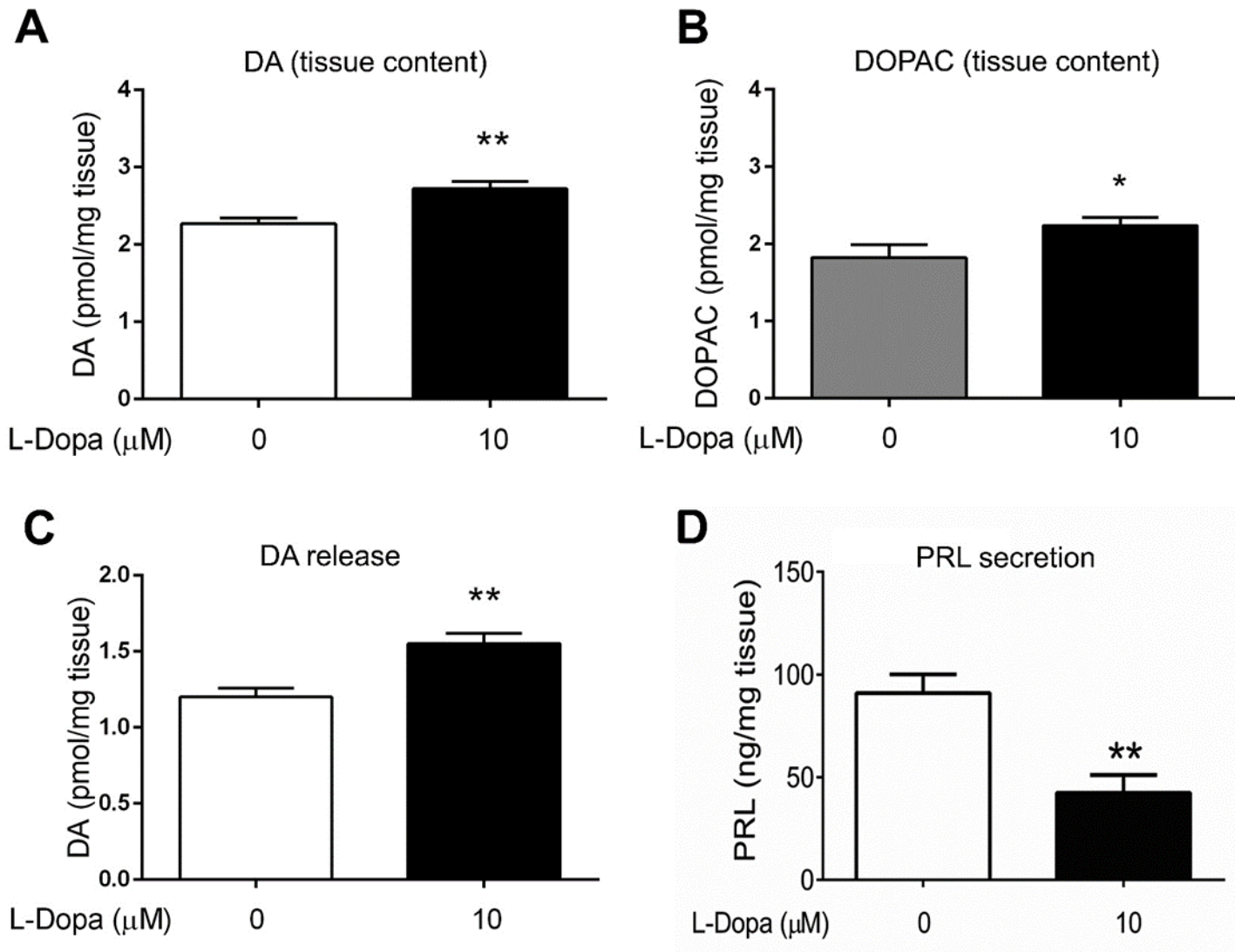


Figure 3. L-Dopa is metabolized in the anterior pituitary gland and plays a potential role in PRL secretion. Each column represents the mean \pm SEM. (A and B) DA and DOPAC tissue levels ($n=7/\text{group}$) were detected by HPLC in anterior pituitary fragments. In the presence of L-Dopa (10 μM) the content of DA and DOPAC was increased. * $p<0.05$ ($t=2.466$ $df=11$), ** $p<0.01$ ($t=3.600$ $df=11$), unpaired t-test. (C) DA was detected by HPLC in conditioned media ($n=6$ wells/group) from anterior pituitary fragments incubated with or without L-Dopa. In the presence of L-Dopa (10 μM) the content of was increased. ** $p<0.01$ ($t=4.029$; $df=10$), unpaired t-test (D) PRL content was detected by ELISA in conditioned media ($n=14$ wells/group) from anterior pituitary fragments incubated with or without L-Dopa (10 μM). ** $p<0.01$ ($t=3.875$ $df=25$), unpaired t-test.

Fig. 4

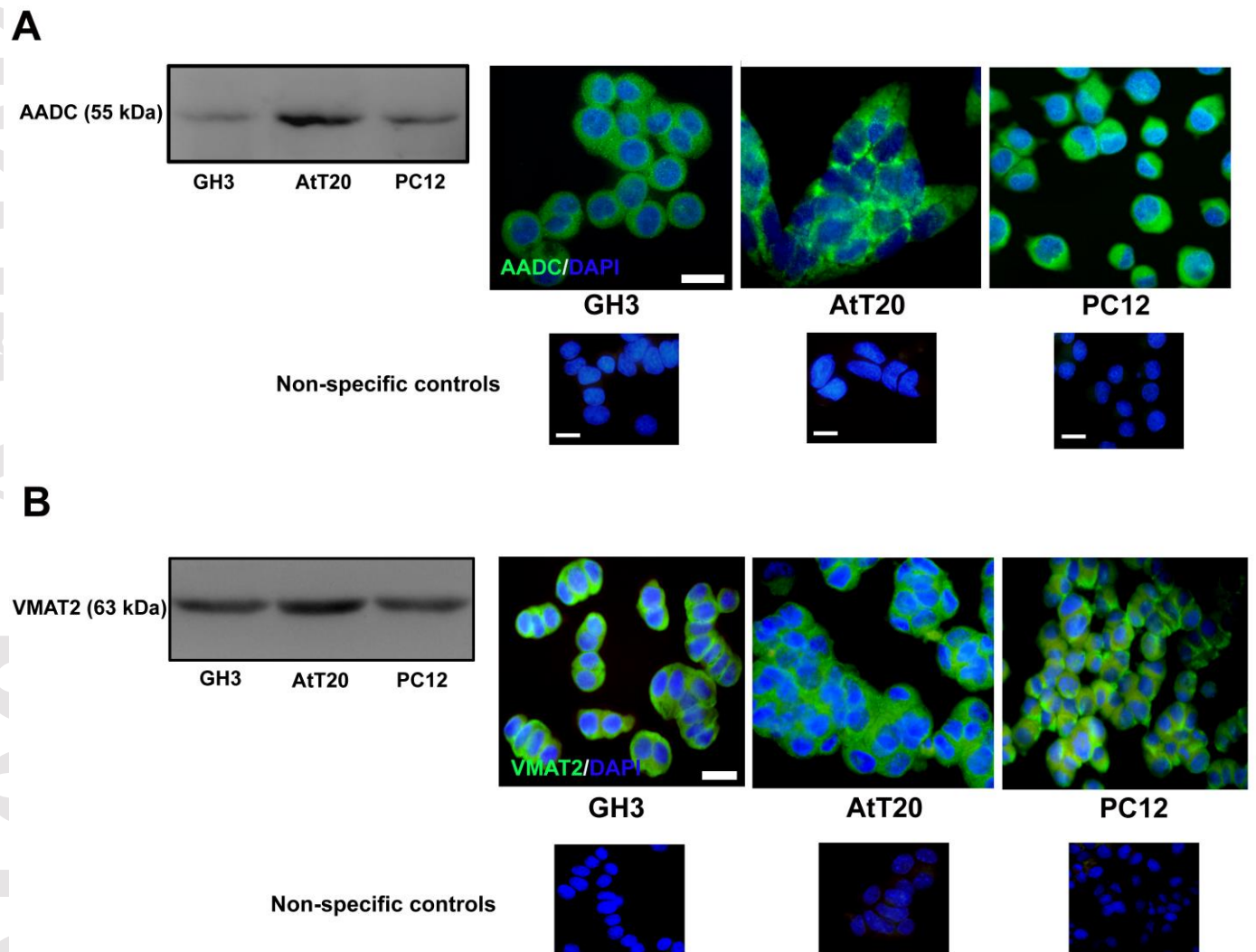


Figure 4. AADC and VMAT2 are expressed in anterior pituitary cell lines. GH3 and AtT20 cells were processed for identification of AADC (A) or VMAT2 (B) by immunofluorescence. Microphotographs show AADC or VMAT2 (green) expression. Nuclei were stained with DAPI (blue). The PC12 cell line was used as a positive control. Results were confirmed by western blot of proteins from GH3, AtT20 and PC12 cells. Scale bars: 20 μ m.

Fig. 5

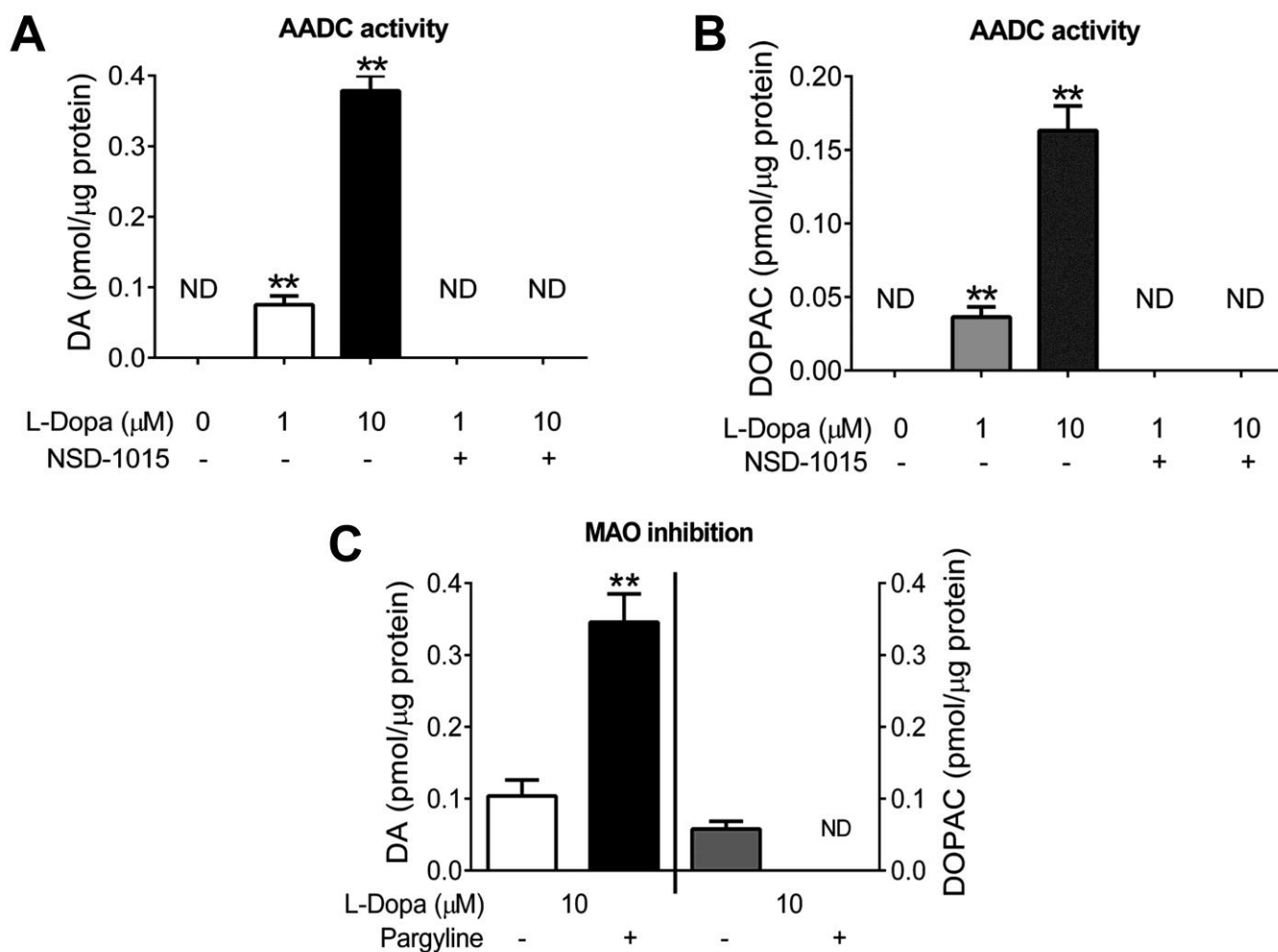


Figure 5. DA and DOPAC are produced from exogenous L-Dopa in AtT20 cells. Each column represents the mean \pm SEM ($n=4/\text{group}$). DA (A) and DOPAC (B) were detected in AtT20 cells by HPLC after incubation with 1 or 10 μM L-Dopa. DA and DOPAC were not detectable (ND) in the presence of NSD-1015. ** $p<0.01$ vs. 0 μM L-Dopa, one-way ANOVA (A: $F(4,15) = 215.9$; B: $F(4,15) = 76.19$) followed by Tukey's test (C) MAO inhibitor (pargyline, 10 μM) prevents the production of DOPAC and increases the content of DA measured by HPLC. ** $p<0.01$ vs. 10 μM L-Dopa without pargyline, unpaired t-test.

Fig. 6

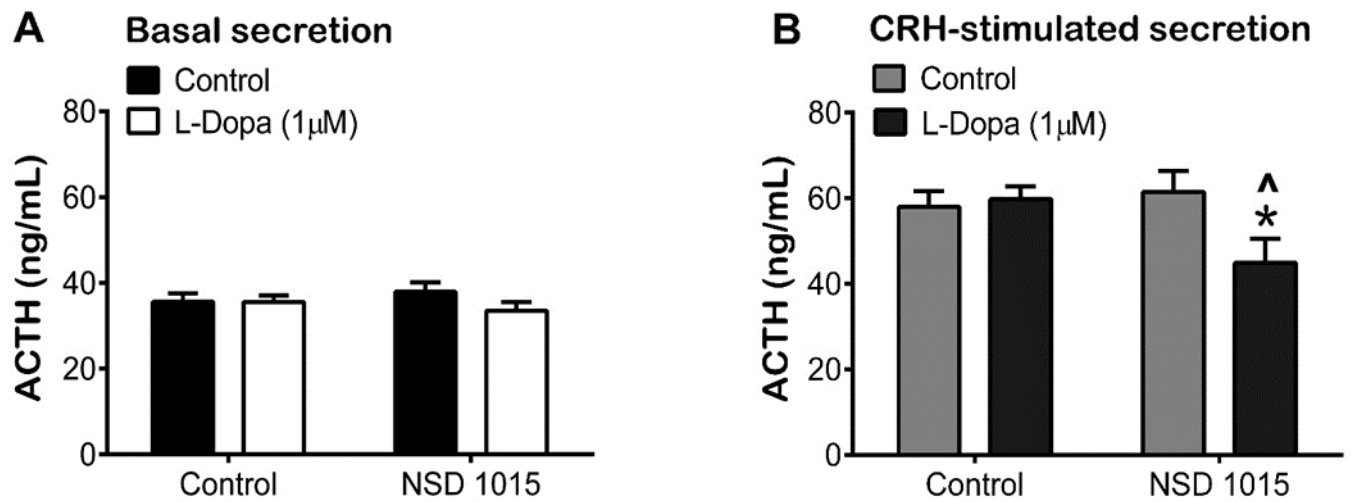


Figure 6. L-Dopa plus an AADC inhibitor reduces CRH-stimulated ACTH secretion from AtT20 cells. Each column represents the mean \pm SEM ($n=9$ /group) of ACTH levels (ng/ml). ACTH was measured in culture media from AtT20 cells by enzyme immunoassay (EIA) both in basal (A) and under CRH (100 nM) stimulated conditions (B). * $p<0.05$ vs. respective controls without L-Dopa, $^{\wedge}p<0.05$ vs. respective control without NSD 1015, two-way ANOVA (A: L-Dopa: $F(1, 32) = 1.339$, $p>0.05$; NSD 1015: $F(1, 32) = 0.005811$; $p>0.05$; Interaction: $F(1, 32) = 1.276$, $p>0.05$). B: L-Dopa: $F(1,31) = 4.749$, $p<0.05$; NSD 1015: $F(1,31) = 0.8971$, $p>0.05$; Interaction: $F(1,31) = 6.789$, $p<0.05$) followed by Newman-Keuls' multiple comparisons test.

Fig. 7

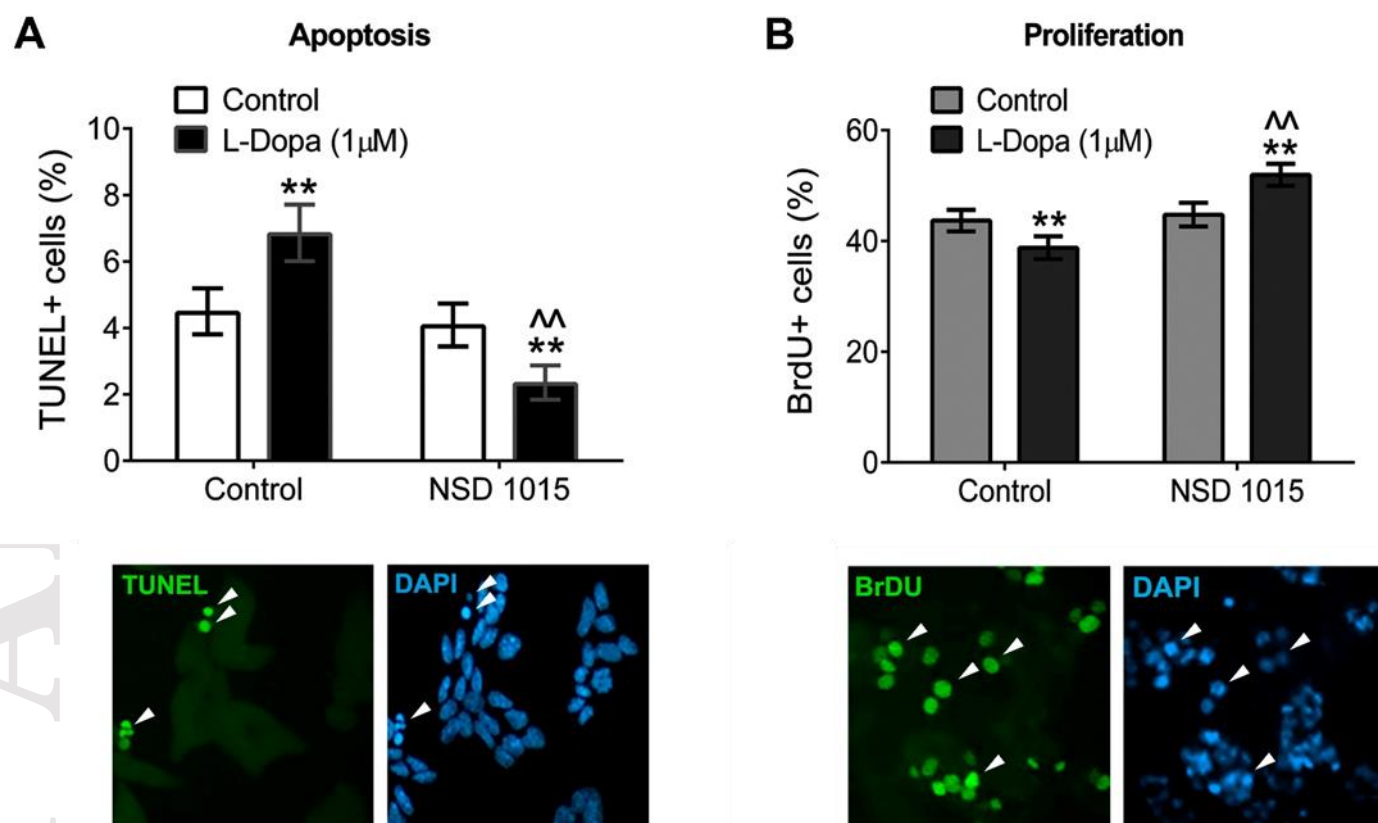


Figure 7. AADC inhibition reverses apoptotic and antiproliferative effects induced by L-Dopa. Each column represents the percentage \pm confidence limit (CL: 95%) of apoptotic (A) or proliferative (B) AtT20 cells ($n \geq 1000$ cell/group) determined by TUNEL or BrdU incorporation assays, respectively. ** $p < 0.01$ vs. respective controls without L-Dopa, ^^ $p < 0.01$ vs respective control without NSD-1015, χ^2 test. Lower panels show representative microphotographs of TUNEL+ or BrdU+ cells (green). Nuclei were stained with DAPI (blue). Arrowheads indicate the location of TUNEL or BrdU positive nuclei. Scale bars: 50 μ m.

Fig. 8

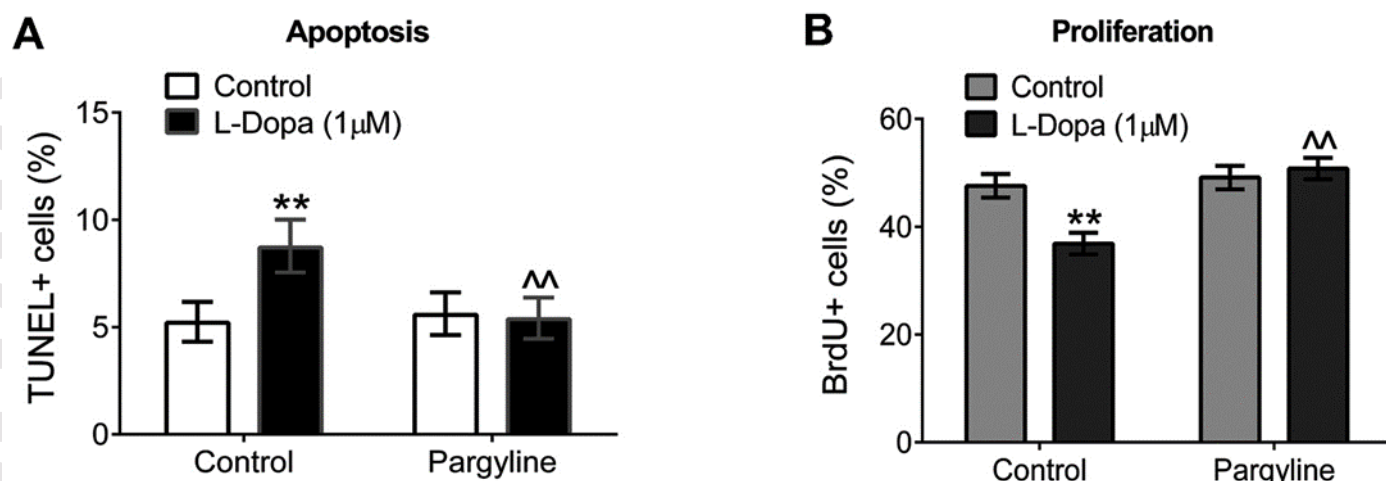


Figure 8. MAO inhibition reverses apoptotic and antiproliferative effects induced by L-Dopa converted to DA. Each column represents the percentage \pm confidence limit (CL: 95%) of apoptotic (A) or proliferative (B) AtT20 cells ($n \geq 1000$ cell/group) determined by TUNEL or BrdU incorporation assays, respectively. ** $p < 0.01$ vs. respective control without L-Dopa, $\wedge p < 0.01$ vs. respective control without pargyline, χ^2 test.